



# Numerical Analysis of the Deformation of a Shearing Machine Tool under Excessive Blade Clearance

Fotios Bantes<sup>1</sup>, George-Christopher Vosniakos<sup>2</sup>, Protesilaos Kostazos<sup>3</sup>

<sup>1</sup> Manufacturing Technology Section, School of Mechanical Engineering, National Technical University of Athens, Heroon Polytechniou 9, 15780 Athens, Greece. Email: mc11031@central.ntua.gr

<sup>2</sup> Manufacturing Technology Section, School of Mechanical Engineering, National Technical University of Athens, Heroon Polytechniou 9, 15780 Athens, Greece. Email: vosniak@central.ntua.gr

<sup>3</sup> Manufacturing Technology Section, School of Mechanical Engineering, National Technical University of Athens, Heroon Polytechniou 9, 15780 Athens, Greece. Email: swing@central.ntua.gr

Received October 05 2020; Revised November 18 2020; Accepted for publication November 18 2020.

Corresponding author: George-Christopher Vosniakos (vosniak@central.ntua.gr)

© 2020 Published by Shahid Chamran University of Ahvaz

**Abstract.** Guillotine shearing machines for metal sheet may be inadvertently operated at increased blade clearance. Typical cases were studied using commercially available finite element software with an explicit solver. Loads causing elastic deformation to the machine structure arise from plastic deformation of the sheet metal being processed, its behavior being modelled by modified Johnson-Cook law. Excessive clearance was found to overload the machine considerably compared to normal clearance, owing to considerable lateral forces. As a result, the guillotine and much less so the base of the machine, undergo oscillatory deformation and the sheet is partly sheared and mostly bent. Such analysis helps the designer understand structural issues of the machine tool in extreme situations and modify the design appropriately.

**Keywords:** Machine tool; Shearing; Sheet metal; Clearance; Structural analysis.

## 1. Introduction

Sheet metal shearing seems to be still unrivalled by laser cutting when it comes to long straight cuts in large production series. Shearing is a simple process employing a stationary and a moving blade, the latter being usually inclined with respect to the former by a rake angle. Thus, the moving blade cuts the metal sheet in a progressive manner. On top of sheet thickness there is a small clearance, thus forming a gap between the blades. The sheet metal is held by a blank holder [1].

The process can be considered to progress in stages involving a failure mechanism with crack propagation, the main parameters being material properties, sheet thickness, blade clearance, cutting edge wear, blank holder force and blade velocity [2]. Blade clearance is a critical parameter. As clearance increases, the volume of the material undergoing shear increases, the resulting sheared surface becomes rougher and the burr formed is more pronounced [3]. Optimum clearance is generally 10-15% of sheet thickness, whereas clearance lower than 5% can lead to secondary shearing. However, more intricate influences may exist for particular materials and setups, e.g. for temperature above 150 °C clearance needs reduction, whereas for ASTM 304 stainless steel optimum clearance is larger than for ASTM 410 steel [4]. As rake angle increases, cutting force decreases [5], but also adversely influences cutting quality by inducing additional deformation on the sheet; therefore it is usually constrained to 3° [6].

Lateral force, amounting to up to 30% of the cutting force, is also exerted on the blade by the sheet being cut [7]. It may result in clearance increase, blade wear and associated quality problems, amplified by rake angle increase [8]. Thus, shearing long sheets involves the risk of large dimensional deviations from one end to the other [9]. Machine tool design has to cater for these factors taking into account machine elasticity.

In this work a hydraulic guillotine shearing machine is considered with a medium range cutting length. These machine tools are intended for cutting large length and width sheets and plates. The stationary blade is fixed to the machine base, whereas the moving blade is attached to a ram moving vertically or pivoting around an axis parallel to the stationary blade. The sheet is held in position by a blank holder. Although analogous machines have already been studied experimentally for rigidity and vibration response [10], this has been done for normal operation mode. In this work, a particular mishandling case by the machine operator is studied numerically, namely setting a clearance much larger than its normal value. Both novice and experienced operators alike may be susceptible, resulting in increased loading which may eventually lead to permanent deformation on the machine structure, as well as to detrimental effects on product quality. Unlike most works that have analysed the process i.e. shearing of the sheet metal, the subject of this work is structural analysis of the machine tool in terms of deformation. The peculiarity of FEA modelling of this situation pertains to the fact that the loads causing elastic deformation to the machine structure arise from plastic deformation of the sheet metal being processed, which required special formulation of the FE model. In Section 2 of this



paper a literature review concerning numerical simulation of shearing and associated processes is given. Section 3 presents the Finite element Model as formulated and implemented on a solver of an explicit type. Section 4 presents and discusses simulation results especially focussing on forces, their influence on the machine and their dependence on various process parameters. Section 5 summarises conclusions and provides cues for future work.

## 2. Literature Review

Essentially all work reported on sheet metal guillotining focuses on process mechanics. The machine tool on which the process is performed has not drawn much attention, if any at all. Of course, modelling of the process is necessary in order to study machine tool deformation, but very few of the papers reviewed have advanced that far.

Finite element formulations have been invariably used to study guillotining. Wisselink [11] constructed a 2D and a 3D model employing a modified Oyane yield criterion based on damage accumulation for small cutting velocity and a pre-existing crack. Arbitrary Lagrangian Eulerian (ALE) formulation was used in order to avoid large deformations and remeshing, with penalty type contacts. Solution on an implicit code took several days deviating from experimental results at large strains. A similar approach in 2D plane strain condition described failure by discrete crack and not by element deletion, resulting in calculation of the cut surface shape as well as cutting force with respect to blade travel [12].

Anisotropic plasticity and isotropic ductile failure were considered in [13], following a Lagrangian formulation with hexahedral and tetrahedral elements with reduced integration in an explicit solver involving Coulomb friction and detachment of failed contact elements between tool and sheet. Cutting force was calculated for both rigid and elastic tools, the difference being around 30%.

Comparison of a 2D and a 3D modelling approach for cutting force calculation concluded that the former can be trusted for faster response, albeit for rigid tooling isotropic elasto-plastic sheet material with exponential hardening, Cockroft-Latham failure model signalling crack onset [14]. Similarly, optimum blade clearance for rigid tooling and ideal plastic material was determined using Cockroft-Latham failure criterion [15].

2D modelling for elastic tools, elastoplastic material and constant acceleration as input employed fully integrated tetrahedral elements, adaptive remeshing, static and dynamic friction on an explicit solver with mass scaling, which was totally acceptable for small accelerations [8].

A number of studies concentrated on blanking instead of guillotining, i.e. on shearing along a closed profile instead of an open line respectively. Numerical modelling of both processes bears high similarity, hence these studies are included in this review.

Early on, analytical cutting force equations considering crack propagation and edge geometry were solved numerically [16]. A little later, the differences between open line inclined blade cutting and closed profile blanking were highlighted, in terms of power being absorbed by shearing and failure in the direction of cutting, blade bending, blank twisting and friction [17].

A simple 2D plane strain FE model using ALE formulation and von Mises yield criterion was validated with experimental data, differences being attributed to neglecting strain rate, anisotropy and friction [18]. A failure criterion according to the maximum hoop stress, maximum principal stress, energy release rate and crack tip angle was employed to study clearance influence on stress at the blade edge [19]. Gurson-Tvergaard-Needleman (GTN) proved superior to the classic elastoplastic model due to its accounting for grain coalescence, failure description by discrete crack method enabling representation of surface quality [20]. A new viscoplastic model and a failure model that had been proposed by Husson including strain rate and temperature effects proved superior to Johnson-Cook  $\kappa$  Gurson models [21] and was employed to prove that as blade clearance increases fracture angle increases and tool wear leads to higher burr, whereas friction does not influence surface quality. Variable clearance for minimising tool wear was proposed in [22] using a numerical study employing no failure model.

High speed blanking was modelled in by a numerical model incorporating strain rate [23] and a 2D quasi-static model with strain rate as well as temperature effects [24], showing increase of maximum force with increasing velocity. A simple elastic linear model was used to study shape aberrations in punching, shearing and slitting in connection to residual stresses [25].

## 3. Finite Element Formulation

The finite element (FE) model constructed had to balance simplicity and accuracy within the LS-dyna solver capabilities following the explicit scheme. The relevant development steps are described next.

### 3.1 Machine tool geometric modelling

The machine tool studied in this work is a Boschert-Gizelis™ model G-Cut CNC 3006, hydraulically powered, see Figure 1(a) and Table 1.

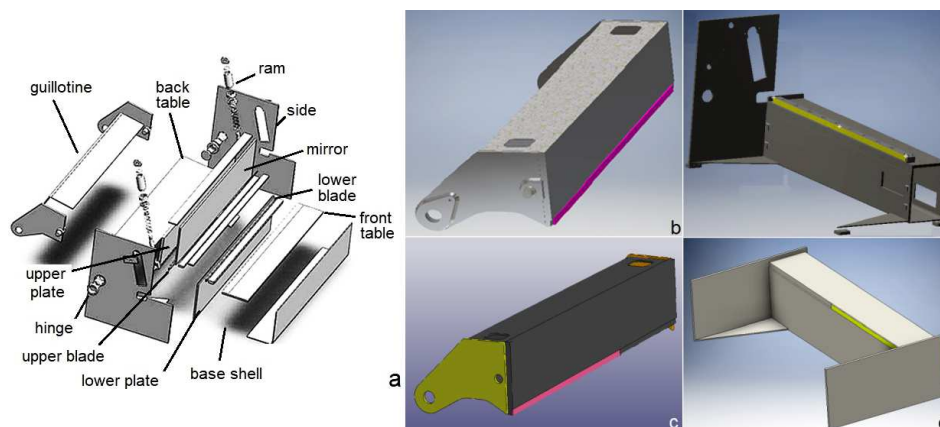


Fig. 1. Machine studied (a) full (b) guillotine CAD model (c) simplified guillotine CAD model (d) base CAD model (e) simplified base CAD model



**Table 1.** Machine tool features

| Feature     | value | Feature                | value | Feature                                 | value |
|-------------|-------|------------------------|-------|---|-------|
| Length (mm) | 3950  | Throat depth (mm)      | 180   | Max cutting thickness (inox steel) (mm) | 4     |
| Height (mm) | 1950  | Back gauge stroke (mm) | 1000  | Max cutting length (mm)                 | 3100  |
| Width (mm)  | 3900  | Weight (kg)            | 8300  | Cutting angle (°)                       | 1.42  |

**Table 2.** Material properties used (nn: not necessary)

|                               | Machine component   |                     |                     |                     |
|-------------------------------|---------------------|---------------------|---------------------|---------------------|
|                               | Sheet               | Guillotine          | Base                | Blades              |
| Material                      | AISI 304            | AISI 305            | AISI 305            | AISI 450            |
| Young's modulus (MPa)         | 195x10 <sup>3</sup> | 195x10 <sup>3</sup> | 195x10 <sup>3</sup> | 220x10 <sup>3</sup> |
| Poisson ratio                 |                     | 0.29                |                     |                     |
| Yield stress (MPa)            | 215                 | 240                 | 240                 | 640                 |
| Strain at failure             | 0.45                | nn                  | nn                  | Nn                  |
| Ultimate Tensile stress (MPa) | 505                 | 620                 | 620                 | 985                 |
| Density (kg/m <sup>3</sup> )  |                     | 7.9x10 <sup>3</sup> |                     |                     |

The sheet interacting with the machine tool is geometrically simple: a plate of dimensions 1500 mm x 200 mm x 2 mm. The machine, on the other hand, comprises a number of elements which are practically impossible to model in the analysis. Therefore, it has to be simplified by keeping only the basic parts: guillotine (moving ram), base (stationary frame), upper (moving) blade, lower (stationary) blade and blank holder. The guillotine and base models are shown in Figure 1(c) to (e), including the pivot area, force application area and base feet. The upper and lower blades are modelled as separate bodies. A radius of curvature of 0.5 mm was used for the blades' cutting edges denoting light wear [13]. The blank holder in reality consists of a number of sequentially placed pneumatic rams in a straight line, but it was simplified as a continuous plate.

Integration in 8-node hexahedral and 4-node tetrahedral elements that were used in this study may be either 'full' or 'one-point'. The former provides greater precision and helps avoiding hour-glassing, but is computationally three times more expensive than one-point integration and also exhibits instability (negative or subcritical valued Jacobian, whilst the total volume is positive) in high deformations. Therefore, one-point integration was preferred at a computational cost associated with their degeneration with zero energy forms.

The guillotine was meshed with medium density tetrahedral instead of hexahedral elements with edge size of about 60 mm, see Figure 2(a). The base is similarly meshed, see Figure 2(b). Evidently, the blades' mesh is much denser than the guillotine's, see Figure 2(c).

Regarding sheet meshing, element size has to be comparable to that of blade elements with which they come into contact, for reasons of contact stability. Given the small elements in the region of curved cutting edge sheet element size of 0.2 mm x 1 mm is set in this area, see Figure 2(d). Furthermore, there should be enough elements across the thickness of the sheet (in this case: 4), since it is expected that stress varies considerably in that direction, at least within a zone of width somewhat larger than the blade clearance, see Figure 2(d). Hexahedral elements were used throughout due to the associated stability compared to tetrahedral elements.

On the blade's curved surfaces 4-element discretisation was selected leading to a maximum dimension of 0,0625 mm, whilst in the direction of the blade's length good resolution is needed not only due to contact and the associated forces but also to monitor its deformation during cutting. Elements are hexahedral but neither structured nor uniform, see Figure 2(e)-(f). Regarding the blank holder the mesh consists of 2D shell elements of relatively large size.

**3.2 Boundary conditions**

The upper blade is fixed on the guillotine. The guillotine is suspended by hinges at the two sides of the base and is subjected to force from the hydraulic rams at both ends, see Figure 1(a). Cutting speed of 750 mm/s was assigned to the nodes at the connection points of the guillotine and the hydraulic cylinder rod. Rolling contact was assigned to the hinge points. The base is fixed on the ground by four screws, see Figure 1(b), the pertinent nodes being assigned zero displacement and rotation. The vertical force exerted on the sheet by the blank holder rams was replaced by a 15 μm vertical displacement for the holder plate, reached directly at simulation start.

**3.3 Material model**

Blade, guillotine and base were modelled as elastic, the blank holder was modelled as rigid and the sheet was modelled as elasto-plastic in connection with a failure criterion. The full Johnson-Cooke model is computationally heavy; moreover, the aim is not to predict with highest accuracy the behaviour of the sheet but to study machine deformation. Thus, a simplified Johnson-Cooke model was applied neglecting temperature effects and dealing with sheet failure through effective plastic strain:  $\sigma_y = A + B(\epsilon^p)^n$  where  $A=215, B=1275, n=0.45$  for inox steel [26]. Material properties used are shown in Table 2.

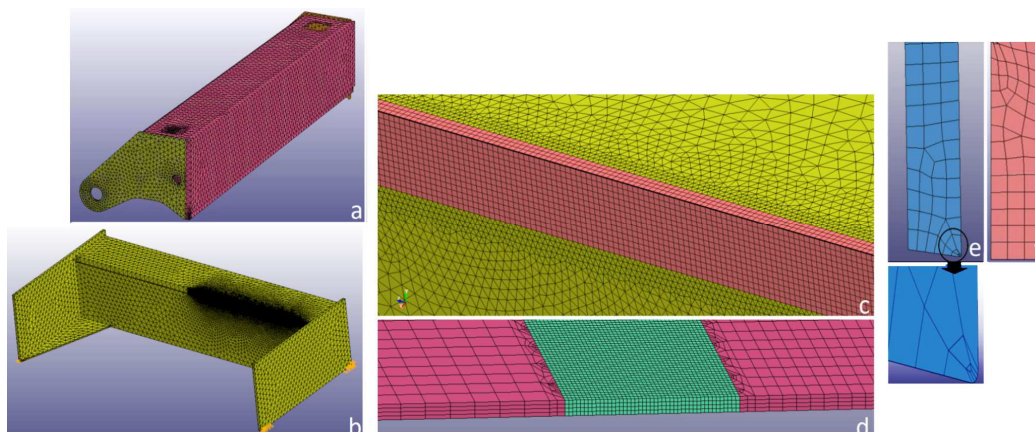


**Fig. 2.** Meshing (a) Guillotine (b) Base (c) Base-blade interface (d) Sheet (e) Upper blade (f) Lower blade



3.4 Contacts

Surface-to-Surface type of contact was preferred, where contact is identified when the slave body's surface nodes penetrate the master body. The pertinent forces are calculated by considering a spring between master and slave nodes and multiplying the pertinent displacement by the spring's constant  $k$ , which is calculated from the compliance of the two bodies. The maximum time step for a stable contact is proportional to  $\min[\sqrt{(m/k)}]$  where  $m$  is the mass on which the contact spring is fixed. Penetration may not be due to the time step but to the resulting elastic constant, in which case  $k$  is increased by using a penalty factor or  $k$  is computed by reference to the time step itself:  $k_{cs}(t) = 0.5 S' m^* / \Delta t_c(t)^2$ , where  $S'$  is the scale factor,  $m^*$  is a function of interfacing nodes masses and  $\Delta t_c$  is the time step. Note that the maximum of  $k_{cs}$  and  $k$  is adopted.

Four kinds of Surface-to-Surface contact were used:

- a) Automatic, where each body's nodes are checked against penetration into the other's, i.e. a symmetrical contact is defined, increasing reliability, but also computational cost
- b) One way, where only the slave node is checked against penetration into the master body; this is applied to the upper blade and the sheet, since their orientation is approximately known beforehand
- c) Eroding surface-to-surface, whereby the elements that fail are deleted from slave search and the interacting parts are determined from scratch, making for costlier, yet sometimes necessary, computation. For instance, when clearance is large, this type of contact is not needed, since the sheet elements coming into contact with the blades are initially not deleted. For small clearance values, this type of contact is preferred to other types, which would lead to instabilities (negative volume) even for small penetration of the edge into the sheet.
- d) Tied, where slave nodes are fixed on the respective master nodes; this is applied to the blade to guillotine connection allowing different materials to be assigned to them.

3.5 Mass scaling

Time step per element is calculated as:  $\Delta t = L_e / c$  where  $L_e$  is the characteristic element length and  $c$  the speed of sound. Time step is determined by the element that results in the lowest value of  $\Delta t$  multiplied by a scale factor. Therefore, to increase the time step one may increase the element size or the material density. Note that, if the mass across the whole model is increased beyond 5%, the results might be unrealistic.

Combining selective mass increase with a meticulous survey of the range of time steps of the model, credible results were reached after some trials. In our case, the smallest elements are found at the sheet and blades. However, the sheet is light and its behaviour can be adversely affected by even a small increase in mass, which effectively limits the time step to  $8.2 \times 10^{-8}$  sec. Very few elements in the transient zone possessed somewhat lower time step value ( $7.588 \times 10^{-8}$  sec). In the base and blades there will be a moderate increase in mass, since comparatively more elements have a time step value lower than that of the sheet, see Figure 3. Note that mass scaling resulted in a dramatic drop in the estimated solution time from 90 h to 30 h.

3.6 Preliminary model validation

Element quality is judged by aspect ratio. Indeed, only one row of elements at the edge of the blade and another two elements at the guillotine side have aspect ratios exceeding the critical value of 5, see Figure 4(a). The same is true about the other blade. As far as the sheet is concerned, see Figure 4(b), very few elements in the highly loaded critical central zone have an inevitably high aspect ratio.

Stress distribution should be compatible with the material model defined. In Figure 4(c) von Mises stress at the beginning of shearing is maximum at the stationary blade edge, as expected due to stress concentration, its value being close to the defined UTS, i.e. around 700 MPa.

Note that kinetic energy at the end of simulation should be lower than internal energy in order to ensure that mass scaling has not introduced undesirable dynamic phenomena.

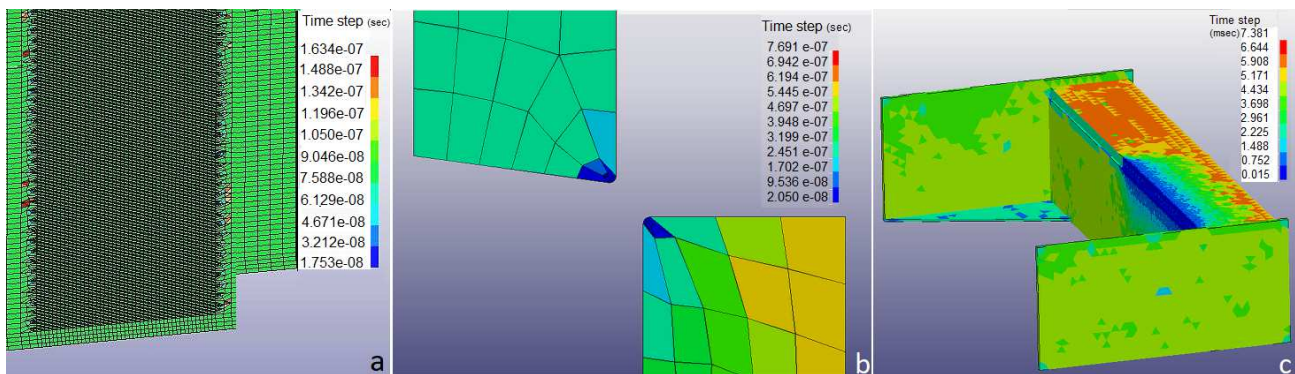


Fig. 3. Time step value distribution (a) sheet (b) blade (c) base

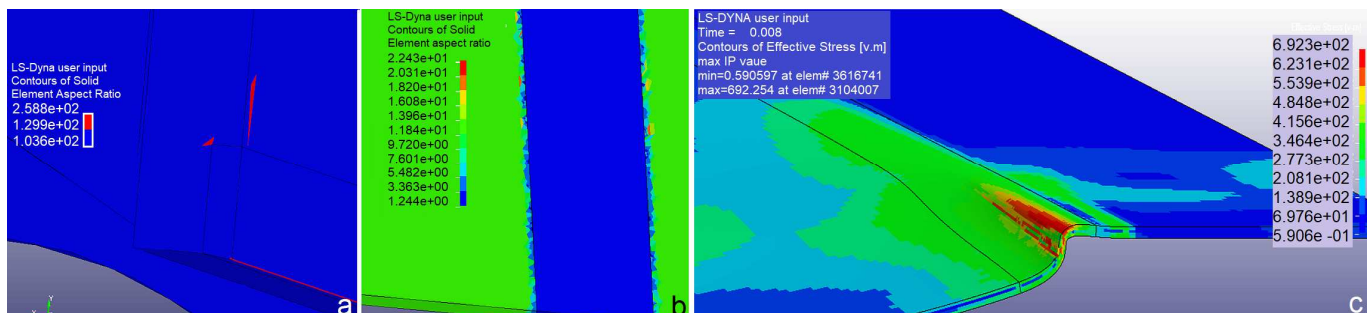


Fig. 4. (a) Blade elements (b) Sheet elements (c) Stress distribution at shearing onset



### 4. Results and discussion

In this study, a clearance of 2.5 mm (blade gap: 4.5 mm) was tried as opposed to the normal clearance equal to 0.2 mm (blade gap 2.2 mm). These cases were compared in terms of forces acting on the guillotine and the base, as well as resulting displacement and its variation in time. In the case of excessive clearance the machine tool was modelled first as deformable and, then, as rigid for the sake of comparison.

#### 4.1 Normal clearance

Shearing mode is depicted in Figure 5, whereas in Figure 6(a) the cutting and lateral forces are shown. The cutting force is relatively stable around 20 kN, showing a peak of 30 kN and decreasing towards the end of the process. This pattern is explained by referring to Figure 7, noting that the latter corresponds to the end of the cutting process (48 – 52 msec). As the blade operates at an angle, it tends to rotate the sheet upon coming into contact with it. Resistance to such rotation leads to the development of a shearing force and is provided by the section of the sheet that has not been cut off yet. At time 50 msec the velocity distribution is compatible with rotation of the sheet about an axis that is normal to the cutting direction and passes near the contact point with the blade. The lateral force applied to the guillotine (as well as to the base) is of particular importance, see Figure 6(a). This is not as stable as the vertical force, reaching, in general, lower values than the latter, except in some points where it exhibits a sharp increase. The respective maxima emerge at the same points in time and along the sheared edge, too.

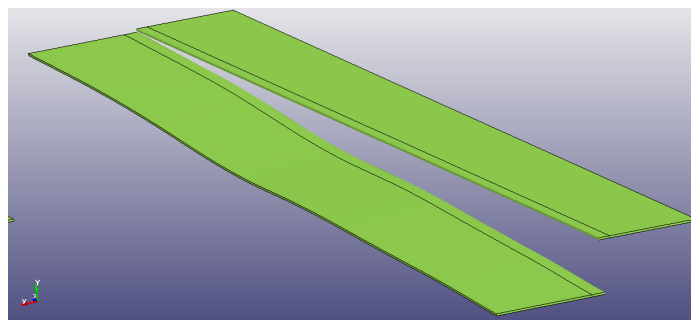


Fig. 5. Sheet shearing with normal clearance and elastic machine

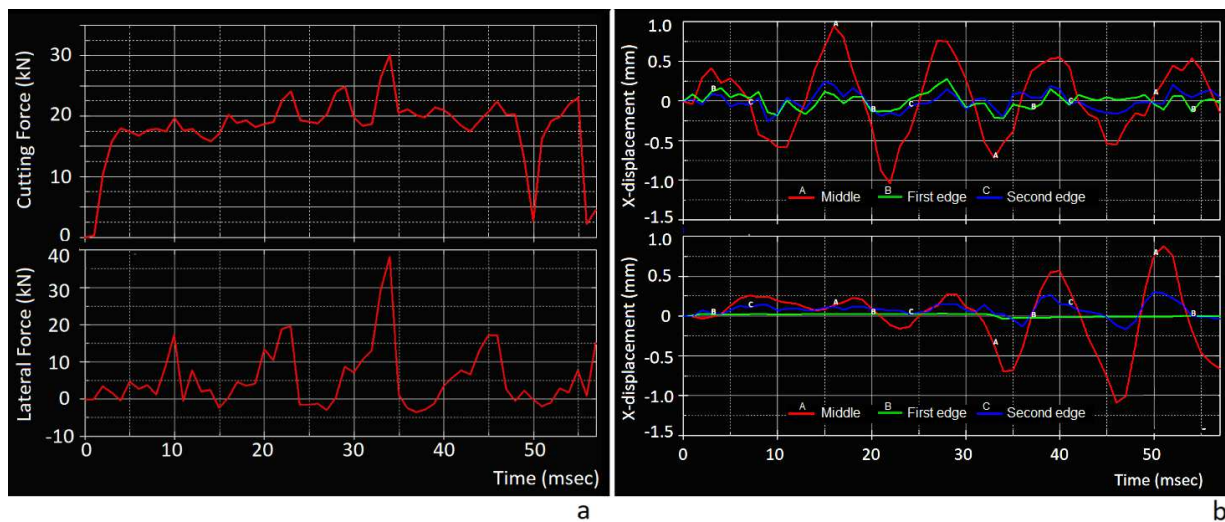


Fig. 6. Normal clearance on deformable machine (a) Cutting and lateral force on upper blade (b) Lateral displacement of middle (A), left end (B), right end (C) points on upper(up) and lower(down) blades

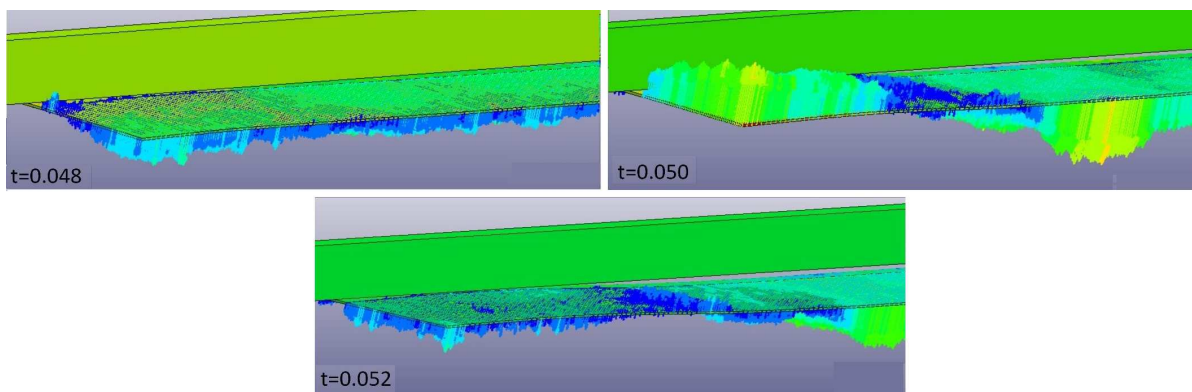


Fig. 7. Normal velocity vectors at the elements of the part to be sheared off



The lateral displacement resulting from machine loading is shown in Figure 6(b). The three points examined correspond to the middle (A), left end (B) and right end (C) of the machine. The guillotine's vibration is noticeable, similar finds having been reported in earlier experimental work [10], [27]. Referring to Figure 6(b) (up), a period of 0.01 sec can be identified, which is in fact the response of the deformable guillotine to the lateral force varying between 0 and 20-40 kN. The mid-point A vibrates four times as much as the endpoints, i.e. oscillatory displacement is about 1 mm. The base's vibration is depicted in Figure 6(b) (down), corresponding to much higher rigidity compared to the guillotine. In fact its displacement at the end points is practically zero, whilst at the mid-point displacement is as low as 10% of the guillotine counterpart. The difference is obviously due to the supports, being just two joints for the guillotine as opposed to the base's full welded sides fixed on the ground.

**4.2 Excessive clearance**

Sheet deformation mode is depicted in Figure 8. Bending is mostly observed, whilst shearing is only partial. In Figure 9(a) the cutting force between sheet and upper blade is shown. Note that the sheet has been modelled as two regions, namely one under high loading and one under low loading. The upper blade first comes into contacts with the first region. As the sheet is being bent, the blade comes into contact, later on, with the second region. Thus, the total force results by summing up forces from both regions. The shearing force keeps on rising up to 159 kN reached at time 20 msec, then slightly varying around 125 kN up to time point 60 msec when it decreases abruptly. This time point corresponds to completion of sheet bending. The low valued force noted thereafter is due to friction between sheet and blade. The lateral force is also shown in Figure 9(a), following a pattern similar to that of the cutting force's. It fluctuates around 125 kN up to the end of shearing. It does not decrease at the end after the material has failed, because high friction causes the sheet to slip off the blank holder, revealing new material under loading.

Johnson-Cook's model allows for strain rate and temperature effects. The latter are considered insignificant, due to the very small duration of the process. The relatively large speed of the latter triggered the strain rate effect to be taken into consideration in a model variation, see Figure 9(b). An increase in normal and lateral forces to a maximum of 192 kN and 208 kN respectively is clear.

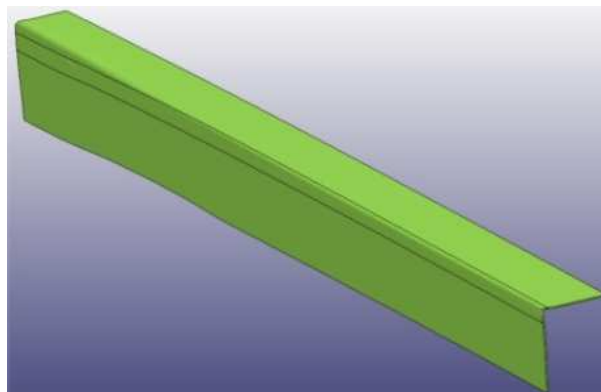


**Fig. 8.** Sheet shearing with excessive clearance and deformable machine

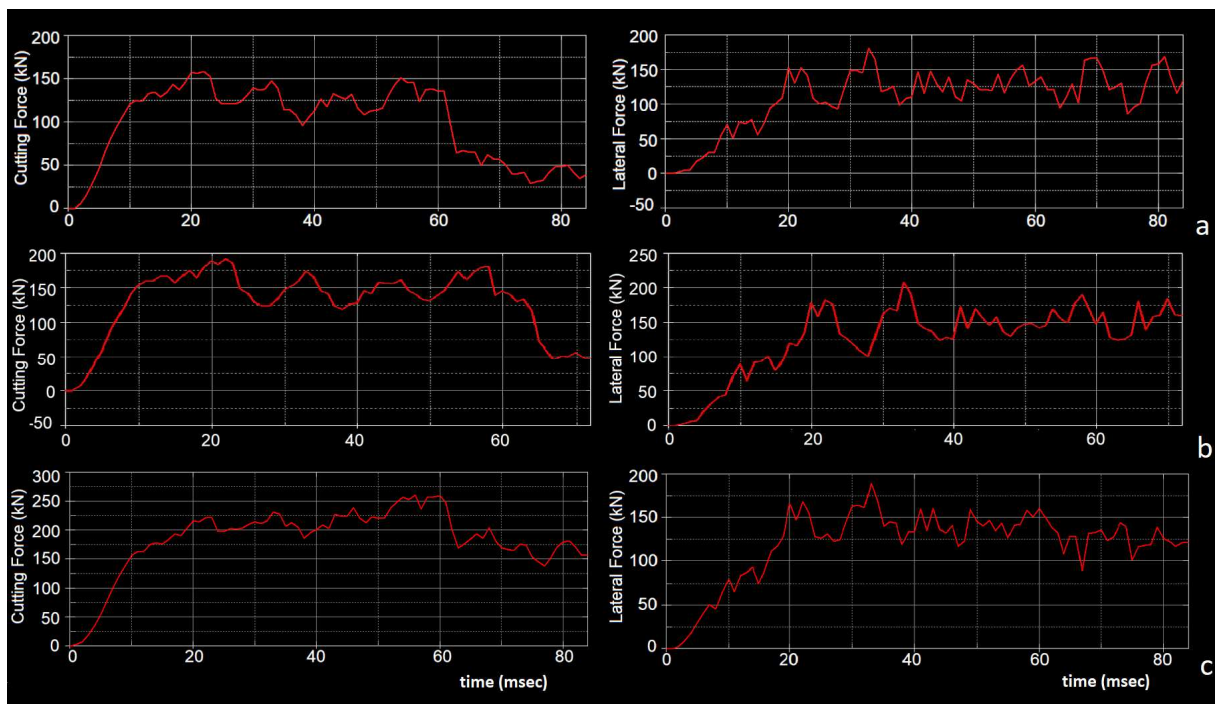


**Fig. 9.** Cutting and lateral force for excessive clearance on deformable machine (a) upper blade (b) upper blade with strain rate effect (c) lower blade



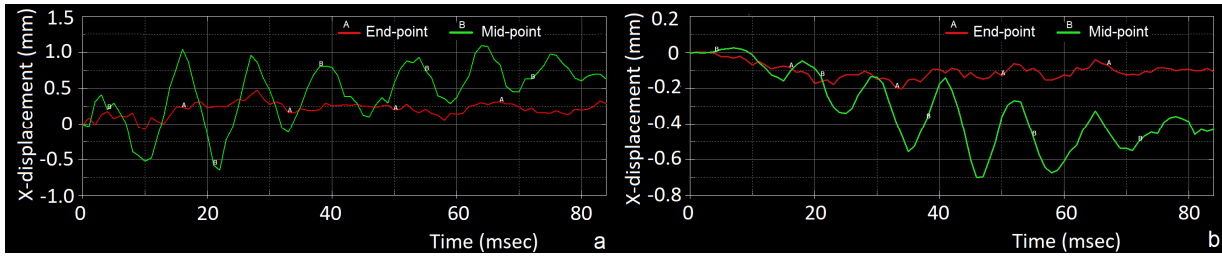


Fig. 10. Displacement of endpoint (A) and midpoint (B) for excessive clearance on deformable machine (a) guillotine (b) base

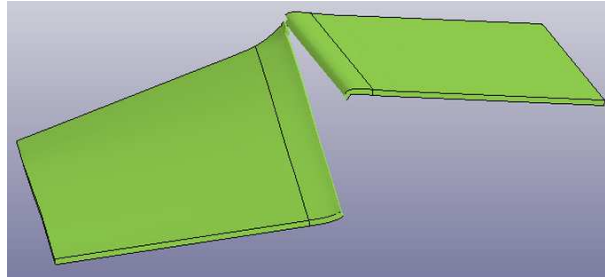


Fig. 11 Sheet shearing with excessive clearance on rigid machine tool

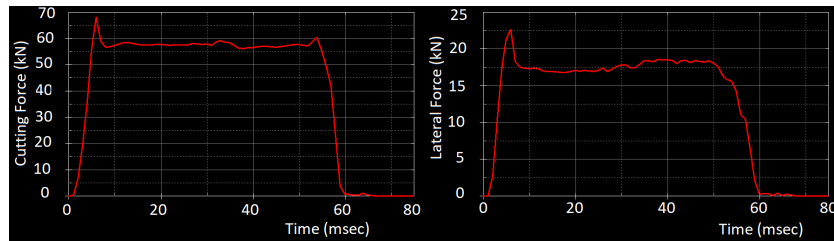


Fig. 12. Cutting and lateral forces on the guillotine with excessive clearance on rigid machine tool

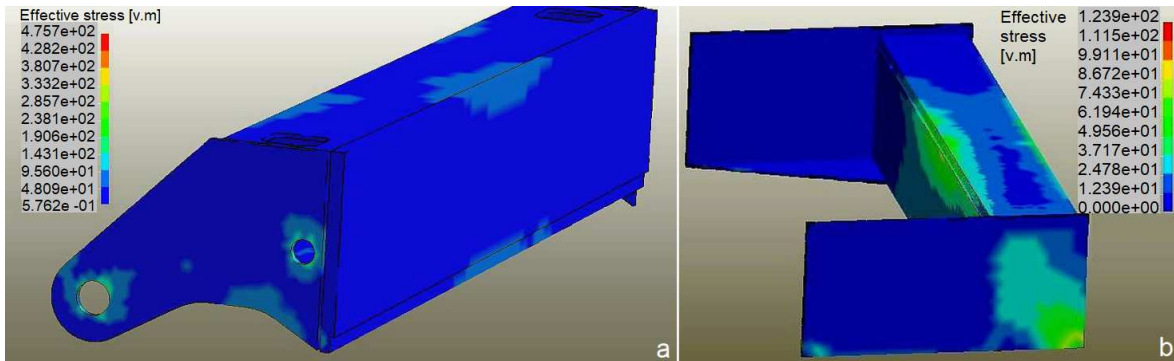


Fig. 13. Worst case of stress distribution (a) guillotine (b) base

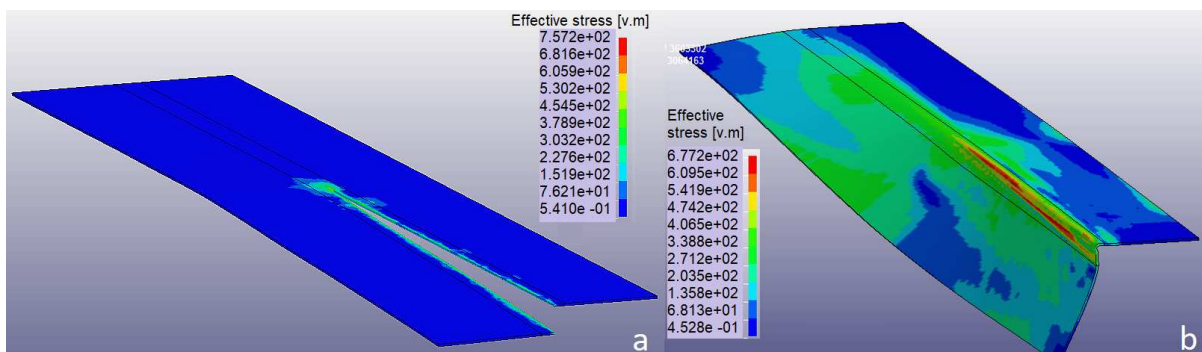


Fig. 14. Stress distribution (a) normal gap of 0.2mm (b) excessive gap of 2.5mm



**Table 3.** Gap influence for deformable machine

| Clearance (mm) | Max Cutting force (kN) |      | Max Lateral force (kN) |      |
|----------------|------------------------|------|------------------------|------|
|                | Guillotine             | Base | Guillotine             | Base |
| 0.2            | 30                     | 35   | 38                     | 14.6 |
| 2.5            | 159                    | 262  | 181                    | 190  |

**Table 4.** Maximum force on guillotine for different models and excessive clearance

|                    | Rigid machine | Deformable machine | Deformable machine<br>incl. strain rate effect |
|--------------------|---------------|--------------------|--|
| Cutting force (kN) | 68            | 159                | 192  |
| Lateral force (kN) | 25            | 181                | 208  |

Figure 9(c) depicts the forces acting on the machine's base. Shearing force reaches a maximum value of 262 kN being kept above 200kN up to time point 60 msec. Thereafter, it decreases moderately, which shows loading being applied by the guillotine through friction with the sheet. Lateral force fluctuates around 135 kN reaching a maximum of 190 kN and slightly decreasing after 60 msec. Note that the non-smooth variation in force is due to both discretisation and the nature of contact (penalty forces).

The lateral displacement of the end-point (A) and mid-point (B) is depicted in Figure 10(a) for the guillotine and in Figure 10(b) for the base. Intense oscillation is conspicuous regarding the midpoint, whereas the endpoint deflects much less. Initially, oscillation happens around zero deflection. However, as the guillotine is lowered and the point of application of the force moves towards the mid-span the guillotine shows a bending deflection, which at the end of shearing is about 0.6 mm. Maximum deflection amounts to 1 mm.

The base deflects in a similar way but to the opposite direction, see Figure 10(b). Deflection at mid-span reaches 0.44 mm at the end of simulation, whereas its maximum value is 0.7 mm. Deflection of the end point is restricted to 0.1 mm. Taking into account the higher loading that it bears, the base is much less compliant than the guillotine.

For comparison, Figure 11 shows that on a non-deformable machine tool the sheet is cut, but non uniformly, whilst it has undergone considerable elongation before failure. The gap remains constant throughout the process, whereas in the case of a deformable machine it increases considerably. As a result, the sheet is sheared more easily. In Figure 12 the shearing and lateral forces are very considerably lower than in Figure 9, reaching a maximum of 68 kN and 25 kN respectively. Forces are also considerably more stable, especially the shearing force.

#### 4.3 Discussion

Maximum loads are exerted on the guillotine at time point 33 msec, when the upper blade has moved vertically by 24.75 mm. This force is applied at an approximate distance of 795 mm from the end of the blade, see Figure 13. The regions in the middle of the guillotine as well as the hinges are shown in lighter colour.

Maximum loads on the base are exerted at time point 60 msec, when the upper blade has moved by a vertical distance of 0.45 mm. This force is applied at an approximate distance of 1375 mm from the end of the blade, see Figure 13. Again, the middle of the base seems to undergo the highest stresses, as well as the rear fixing point at the side where shearing begins.

Comparison of cutting and lateral forces for normal and excessive clearance can be made by referring to Figure 9 and Figure 6. Forces in the case of excessive clearance are markedly larger, since in that case the whole of the sheet contributes to accumulating force, whereas for normal clearance the sheet part that has failed does not have any contribution. A summary of the influence of clearance to the maximum force observed is given in Table 3.

A summary of the differences due to the modelling assumptions is given in Table 4. Note that an increase in clearance also signifies an increase in the area undergoing shearing. This is clearly depicted in Figure 14, showing the stress distribution in both cases corresponding to the same point in time. Partial shearing in the case of excessive clearance can be observed.

## 5. Conclusions

In this work the case where excessive blade clearance is set on a guillotine-type shearing machine was studied numerically. This is a possibility that is due to reckless use, but nevertheless, it has to be taken into account by the machine designers. The aim was to calculate the emerging forces and the repercussions for the machine's accuracy and ultimately its structural health. This was achieved by suitable simplified modelling of the machine tool's geometry to allow the finite element solver to yield credible results in reasonable time. A particular machine was studied, but conclusions are general enough. In designing the machine to withstand loading, the lateral force magnitude cannot be neglected, since it is comparable to the cutting force. Indeed, it was found that an excessive clearance causes multiplication of forces acting on the machine by a factor as high as 4 compared to normal clearance. As a result, the guillotine and the base of the machine exhibit significant non-uniform displacement, of several tens of a mm. This impacts the quality of the sheared edge of the sheet, especially since the displacement is not uniform along the edge. In addition, if this happens repeatedly, permanent deformation of the machine may result which may render the machine unusable. Future extension of the work as far as computational mechanics is planned in order to determine the influence of shearing speed and especially blade wear. It may also provide an estimate as to the number of loading cycles that lead to permanent deformation of the machine, especially taking into account the welding process parameters used to construct the machine's components [28], such as guillotine, base shell etc. In terms of experimental validation of the numerical model, it is aimed to use strain gages at selected points of the structure as well as capacitive sensors at several points along the blades following the approach demonstrated in [29]. However, this should be restricted to normal clearance (gap) in order to avoid detrimental effects to the machine structure associated with excessive clearance, as clearly demonstrated in the present work.

### Author Contributions

F. Bantes set up the FEA model and conducted the executions, G-C. Vosniakos initiated the project, analyzed the results and wrote up the manuscript and P. Kostazos supervised the FEA work and debugged the model as necessary. All authors reviewed and approved the final version of the manuscript.

### Conflict of Interest

The authors declared no potential conflicts of interest with respect to the research, authorship, and publication of this article.



## Funding

The authors received no financial support for the research, authorship, and publication of this article.

## References

- [1] Wu, X., Bahmanpour, H., Schmid, K., Characterization of mechanically sheared edges of dual phase steels, *Journal of Materials Processing Technology*, 212(6), 2012, 1209–1224.
- [2] Maiti, S.K., Ambekar, A.A., Singh, U.P., Date, P.P., Narasimhan, K., Assessment of influence of some process parameters on sheet metal blanking, *Journal of Materials Processing Technology*, 102(1-3), 2000, 249–256.
- [3] Kibe, Y., Okada, Y., Mitsui, K., Machining accuracy for shearing process of thin-sheet metals-Development of initial tool position adjustment system, *International Journal of Machine Tools and Manufacture*, 47(11), 2007, 1728–1737.
- [4] Ma, L. Feng, Huang, Q.X., Huang, Z., Chu, Z.B., Tian, Y.Q., Establishment of Optimal Blade Clearance of Stainless Steel Rolling-Cut Shear and Test of Shearing Force Parameters, *Journal of Iron and Steel Research International*, 19(9), 2012, 52–61.
- [5] Gustafsson, E., Karlsson, L., Oldenburg, M., Experimental study of forces and energies during shearing of steel sheet with angled tools, *International Journal of Mechanical and Materials Engineering*, 11(1), 2016, 10.
- [6] Mackensen, A., Golle, M., Golle, R., Hoffmann, H., Experimental investigation of the cutting force reduction during the blanking operation of AHSS sheet materials, *CIRP Annals*, 59(1), 2010, 283–286.
- [7] Kopp, T., Stahl, J., Demmel, P., Tröber, P., Golle, R., Hoffmann, H., Volk, W., Experimental investigation of the lateral forces during shear cutting with an open cutting line, *Journal of Materials Processing Technology*, 238, 2016, 49–54.
- [8] Gustafsson, E., Oldenburg, M., Jansson, A., Design and validation of a sheet metal shearing experimental procedure, *Journal of Materials Processing Technology*, 214(11), 2014, 2468–2477.
- [9] Yoshida, Y., Elastic clearance change in axisymmetric shearing process, in: *Proceedings of the 19th International ESAFORM Conference on Material Forming*, 27–29 April 2016, Nantes, France, (eds: F. Chinesta, E. Cueto, E. Abisset-Chavanne) AIP Conference Proceedings 1769, (1), 150003, 2016 (online), AIP Publishing LLC.
- [10] Ramamurti, V., Sasikiran, S., Vinod Kumar, P., Dynamic analysis of a guillotine shearing machine, *Journal of Materials Processing Technology*, 71(2), 1997, 202–214.
- [11] Wisselink, H.H., *Analysis of guillotining and slitting, finite element simulations*, Ph.D. Thesis, Department of Mechanical Engineering, University of Twente, 2000.
- [12] Brokken, D., Brekelmans, W.A.M., Baaijens, F.P.T., Numerical modelling of the metal blanking process, *Journal of Materials Processing Technology*, 83(1-3), 1998, 192–199.
- [13] Saanouni, K., Belamri, N., Autesserre, P., Finite element simulation of 3D sheet metal guillotining using advanced fully coupled elastoplastic-damage constitutive equations, *Finite Elements in Analysis and Design*, 46(7), 2010, 535–550.
- [14] Berti, G.A., Monti, M., Numerical modelling of sheet metal guillotining process, in *Proceedings of the 13. Round Table: Simulation in der Umformtechnik*, (ed.M. Wohlmut) 23–25 April 2012, Bamberg, Germany, 262–271.
- [15] Li, Y.G., Ye, Q., Fan, F., Bao, Y., Huang, Q.X., Finite Element Method Analysis of Effect of Blade Clearance on Plate Shearing Process, *Journal of Iron and Steel Research International*, 19(10), 2012, 26–29.
- [16] Atkins, A.G., On cropping and related processes, *International Journal of Mechanical Sciences*, 22(4), 1980, 215–231.
- [17] Atkins, A.G., On the mechanics of guillotining ductile metals, *Journal of Materials Processing Technology*, 24, 1990, 245–257.
- [18] Stegeman, Y.W., Goijaerts, A.M., Brokken, D., Brekelmans, W.A.M., Govaert, L.E., Baaijens, F.P.T., An experimental and numerical study of a planar blanking process, *Journal of Materials Processing Technology*, 87(1-3), 1999, 266–276.
- [19] Yu, S., Xie, X., Zhang, J., Zhao, Z., Ductile fracture modeling of initiation and propagation in sheet-metal blanking processes, *Journal of Materials Processing Technology*, 187, 2007, 169–172.
- [20] Lemiale, V., Chambert, J., Picart, P., Description of numerical techniques with the aim of predicting the sheet metal blanking process by FEM simulation, *Journal of Materials Processing Technology*, 209(5), 2009, 2723–2734.
- [21] Husson, C., Correia, J.P.M., Daridon, L., Ahzi, S., Finite elements simulations of thin copper sheets blanking: Study of blanking parameters on sheared edge quality, *Journal of Materials Processing Technology*, 199(1-3), 2008, 74–83.
- [22] Subramonian, S., Altan, T., Ciocirlan, B., Campbell, C., Optimum selection of variable punch-die clearance to improve tool life in blanking non-symmetric shapes, *International Journal of Machine Tools and Manufacture*, 75, 2013, 63–71.
- [23] Marouani, H., Ben Ismail, A., Hug, E., Rachik, M., Numerical investigations on sheet metal blanking with high speed deformation, *Materials and Design*, 30(9), 2009, 3566–3571.
- [24] Subramonian, S., Altan, T., Campbell, C., Ciocirlan, B., Determination of forces in high speed blanking using FEM and experiments, *Journal of Materials Processing Technology*, 213(12), 2013, 2184–2190.
- [25] Bolt, P.J., Sillekens, W.H., Prediction of shape aberrations due to punching, shearing and slitting, *Journal of Materials Processing Technology*, 103(1), 2000, 87–94.
- [26] Kalpakjian, S., Schmid, S.R., Musa, H., *Manufacturing Engineering and Technology*, Prentice Hall, Singapore- London, 2010.
- [27] Ramamurti, V., Rajaram, H., Balasubramaniam, M., Dynamic analysis of two types of over-crank guillotine shears—a comparative study, *Journal of Materials Processing Technology*, 83(1-3), 1998, 54–61.
- [28] Zavidoveev, A., Rogante, M., Poznyakov, V., Heaton, M., Acquier, P., Kim, H.S., Baudin, T., Kostin, V., Development of the PC-GMAW welding technology for TMCP steel in accordance with welding thermal cycle, welding technique, structure, and properties of welded joints, *Reports in Mechanical Engineering*, 1(1), 2020, 26–33.
- [29] Fragassa, C., Minak, G., Pavlovic, A., Measuring deformations in the telescopic boom under static and dynamic load conditions, *Facta Universitatis Series: Mechanical Engineering*, 18(2), 2020, 315–328.

## ORCID iD

Fotios Bantes  <https://orcid.org/0000-0002-9752-3603>

George-Christopher Vosniakos  <https://orcid.org/0000-0002-4484-8359>

Protesilaos Kostazos  <https://orcid.org/0000-0002-3897-2185>



© 2020 by the authors. Licensee SCU, Ahvaz, Iran. This article is an open access article distributed under the terms and conditions of the Creative Commons Attribution-NonCommercial 4.0 International (CC BY-NC 4.0 license) (<http://creativecommons.org/licenses/by-nc/4.0/>).

How to cite this article: Bantes F, Vosniakos G.-C., Kostazos, P. Numerical Analysis of the Deformation of a Shearing Machine Tool under Excessive Blade Clearance, *J. Appl. Comput. Mech.*, 7(2), 2021, 496–504. <https://doi.org/10.22055/JACM.2020.35301.2623>

